



International Conference on Recent Advancement in Air Conditioning and Refrigeration, RAAR
2016, 10-12 November 2016, Bhubaneswar, India

Numerical analysis of a modified type pulse tube refrigerator

Sachindra Kumar Rout^{a*}, Arun Kumar Behura^b, Sisir Dalai^c and Ranjit Kumar Sahoo^c

^aAssistant Professor, C.V.Raman College of Engineering, Department of Mechanical Engineering, Bhubaneswar 752054, India

^bAssociate Professor, Poornima College of Engineering, Department of Mechanical Engineering Jaipur, Rajasthan

^cNational Institute of Technology, Rourkela, Odisha, India

Abstract

The loss generated due to direct current gas flow in pulse tube refrigerator (PTR) is one of the major problems which significantly affect the cooling performance. It generates temperature fluctuation at the cold end of the PTR. A new type PTR has been proposed in the present work to diminish the DC flow problem by attaching an additional connection at the hot end from a secondary compressor and investigated numerically using CFD simulation software FLUENT. It is reported a significant enhancement of cooling performance by means of the proposed model. The numerical outcomes of the proposed model are equated with the outcomes of the orifice type pulse tube refrigerator (OPTR) model. The model used for analysis is an axisymmetric model. At 34 Hz operating frequency and 1.2 pressure ratio the numerical simulation is conducted. The proposed model achieves a temperature of 98 K at cold end where as a simple OPTR having same dimension reaches a temperature of 130 K. To get an optimum result experimentally for the pulse tube refrigerator, is a very difficult and also high expensive hence the numerical approach is an alternate solution.

© 2017 The Authors. Published by Elsevier Ltd. This is an open access article under the CC BY-NC-ND license

(<http://creativecommons.org/licenses/by-nc-nd/4.0/>).

Peer-review under responsibility of the organizing committee of RAAR 2016.

Keywords: MPTR; pulse tube; DC gas flow; orifice.

1. Introduction

Due to the close circuit between hot end heat exchanger and aftercooler through a by pass, there is a positive direct current flow (DC flow) inside the double inlet Pulse tube refrigerator. There are two types DC flow, positive

* Corresponding author. Tel.: +91-8895815648; fax: +0-000-000-0000 .

E-mail address: sachindra106@gmail.com

DC flow and the negative DC flow. The major problem associated with the DC flow is that temperature instability at the cold end due to the circulating steady flow around the aftercooler, regenerator, cold heat exchanger, hot heat exchanger and the pulse tube develops an extra heat load to the cold heat exchanger. This result deteriorates in the

Nomenclature

C_p	specific heat gas constant, (J/kg-K)
C	inertial resistance (m^{-1})
E	overall energy (JKg^{-1})
h	specific enthalpy (J/kg)
k	thermal conductivity (W/m-K)
p	pressure (N/m^2)
t	time (s)
T	temperature (K)
V	volume (m^3)
v	velocity (m/s)

Greek Symbol

ϖ	permeability tensors term (m^2)
τ	stress tensors term (N/m^2)
ρ	density (kg/m^3)
ν	kinematic viscosity
τ	stress tensors (N/m^2)
ϕ	porosity
ω	angular frequency (rad/s)
μ	dynamic viscosity ($kg/m\ s$)

Subscripts

f	fluid
S	solid
z	frequency

performance of a pulse tube refrigerator. Due to convective heat loss [1] direct current flow deteriorates the performance of the PTR. The convective loss causes temperature fluctuation at the cold end which is additional negative influence owed to DC flow. By diminishing the DC gas flow or by breaking the flow circuit due to the by pass the performance of the PTR can be enhanced. There are few works has been reported to eliminate DC flow loss by investigators which are shortened here. Inertance type pulse tube refrigerator (ITPTR) [2-4] and active buffer pulse tube refrigerator (ABPTR) [5-8] can diminish the direct current flow and can provide a greater performance but they have their own limitations. As there are numbers of valve used in ABPTR, it makes complicity in configuration and short life span compare to other type pulse tube refrigerator. The ITPTR model has the limitation that it cannot achieve much lower temperature compare to the DIPTR mode. Different approaches have been proposed by many researchers to suppress the DC flow such as Double-orifice pulse tube refrigerator [9] and the multi-bypass PTR [10] but unable to completely finish it. Membrane suppressor method proposed by Hu [11] et al gives a better solution to DC flow which can completely solve the DC flow loss. The closed-loop flow path generated due to the bypass is break by a use of membrane. An innovative barrier method of a limp rubber balloon was proposed by Swift et al. [12] to solve DC flow problem. This can diminishes the DC flow inside the loop path in a thermos-acoustic Starling cryocooler. Shiraishi and Murakami [13] experimentally manufactured and tested a diaphragm inserted in the bypass-tube which completely diminishes the DC flow. From the literature survey it is reported that there is no numerical work found in this DC flow suppression type pulse tube refrigerator. Using ANSYS FLUENT software package an innovative method is proposed and numerically solved to study the transport phenomenon of a MPTR. In this proposed modeling an axisymmetric model is established by using a supplementary compressor input at the hot end heat exchanger as a substitute of the double inlet valve which purpose is equivalent to difragram function. This can disruption the bypass of a DIPTR as difragram performs. Fig. 1 shows the schematic diagram of (a) OTPTR (b) DIPTR (c) MPTR.

2. Methodology

2.1. Strategy explanation

The detail investigation on MPTR is conducted by the use of CFD simulation software package FLUENT. Fig. 1(c) shows the schematic diagram of the proposed MPTR. As discussed earlier due to the bypass the main DC flow loss is formed which causes temperature unsteadiness near the cold end heat exchanger of the PTR. To avoid such problem the bypass should break and an alternative design is adopted, which perform same benefits, an additional compressor is attached in place of bypass having the same mass flow rate as flows through the bypass.

2.2. Governing Equations and Modelling

A 2D axisymmetric unsteady model is used in the present analysis. The governing equations like continuity equation, momentum equations in both axial and in radial direction and energy equation for solid matrix inside the porous region are solved. To calculate momentum losses two separate source terms, both in axial and in radial direction are included for the porous region. The source term value is zero for the solids, rest of porous medium and solid matrix inside the porous region is considered as homogeneous.

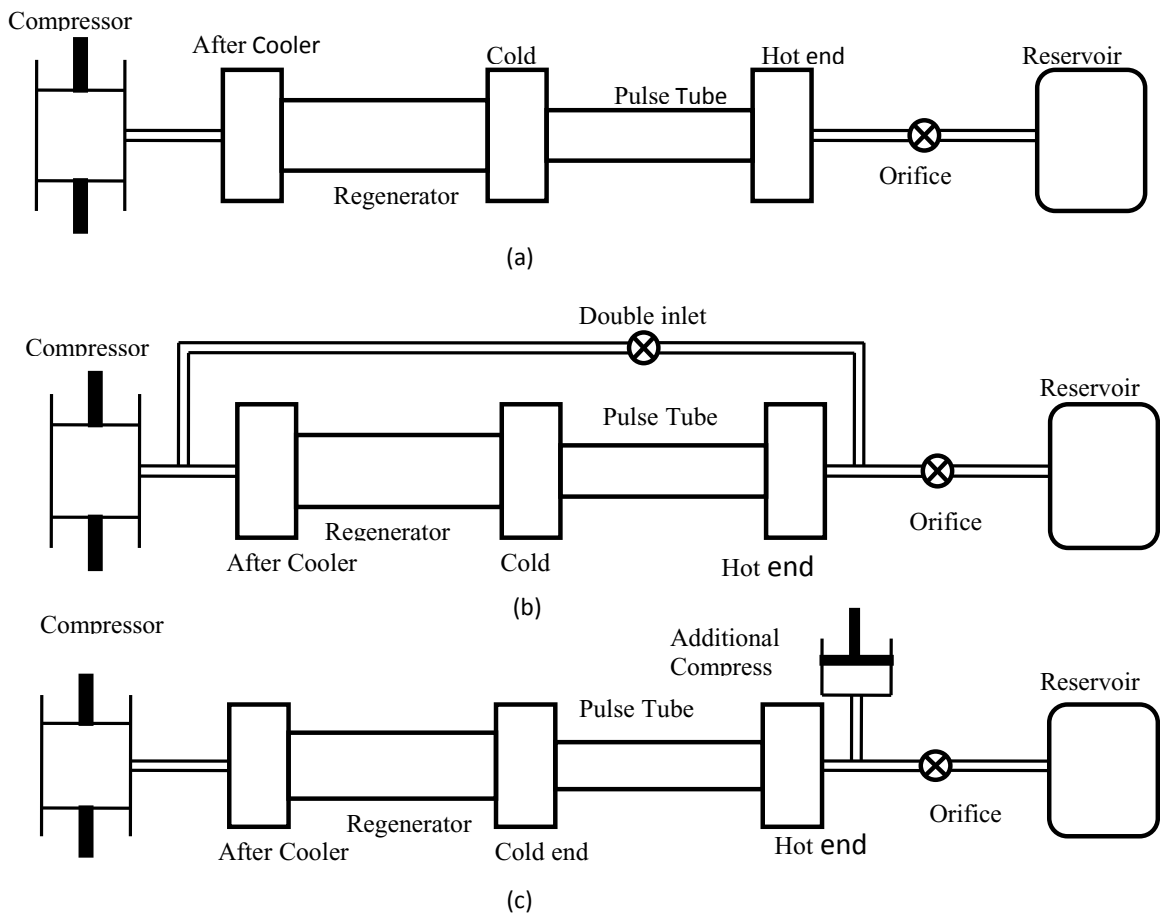


Fig.1 Schematic diagram of (a) OPTR (b) DIPTR (c) MPTR

Continuity Equation

$$\frac{\partial}{\partial t}[\phi\rho] + \nabla(\rho\bar{u}) = 0 \quad (1)$$

Momentum Equations in axial and radial direction:

For the axial direction

$$\begin{aligned} \frac{1}{y} \frac{\partial}{\partial x} [\phi r v_x v_y] + \frac{1}{y} \frac{\partial}{\partial y} [\phi y \rho_f v_x v_y] + \frac{\partial}{\partial t} [\phi \rho v_x] &= \frac{1}{y} \frac{\partial}{\partial y} \left\{ y \mu \left[\frac{\partial \phi v_x}{\partial y} + \frac{\partial \phi v_y}{\partial y} \right] \right\} \\ \frac{1}{y} \frac{\partial}{\partial y} \left\{ y \mu \left(2 \frac{\partial \phi v_x}{\partial x} - \frac{2}{3} (\vec{\nabla} \phi \cdot \vec{v}) \right) \right\} &- \frac{\partial \phi p}{\partial y} + S_x \end{aligned} \quad (2)$$

For the radial direction

$$\begin{aligned} \frac{1}{y} \frac{\partial}{\partial x} [\phi r v_x v_y] + \frac{1}{y} \frac{\partial}{\partial y} [y \phi \rho_f v_y v_y] + \frac{\partial}{\partial t} [\phi \rho_f v_y] &= \\ \frac{2\mu}{y} \left[\frac{(\vec{\nabla} \cdot \vec{v})}{3} - \frac{v_y}{y} (\vec{\nabla} \cdot \vec{v}) \right] + \frac{1}{r} \frac{\partial}{\partial x} \left\{ 2x \mu \left(\frac{\partial v_x}{\partial x} - \frac{1}{3} (\vec{\nabla} \cdot \vec{v}) \right) \right\} &+ \\ \frac{1}{y} \frac{\partial}{\partial y} \left\{ 2y \mu \left[\frac{\partial v_x}{\partial y} - \frac{1}{3} (\vec{\nabla} \cdot \vec{v}) \right] \right\} &- \frac{\partial p}{\partial y} + S_y \end{aligned} \quad (3)$$

The source terms value along the radial and axial direction for the porous zone are S_x and S_y , and zero for nonporous zone. Along the porous zone the source term is defined as following expressions:

$$\begin{aligned} S_x &= -\frac{1}{2} \left(\frac{2\mu}{\sigma} v_x + v_x |v| C \rho_f \right) \\ S_y &= -\frac{1}{2} \left(\frac{2\mu}{\sigma} v_y + v_y |v| C \rho_f \right) \end{aligned} \quad (4)$$

The first term in the above equation is refer to the Darcy term and next term is refer to the Forchheimer term. The pressure drop can be accountable for the porous zone by using the above equations.

Energy Equation:

$$\frac{\partial}{\partial t} (\vec{\nabla} \cdot (\vec{v} (\rho_f E_f + p))) + \phi \rho E_f + (1 - \phi) \rho_s E_s + \vec{\nabla} \cdot (k \vec{\nabla} T_f + \tau \cdot \vec{v}) \quad (5)$$

Where

$$k = \phi k_f + (1 - \phi) k_s \quad (6)$$

$$E_f = h - p / \rho_f + v^2 / 2 \quad (7)$$

2.3. Initial and Boundary Conditions

The formulated governing equations for 2D axisymmetric model are solved using Fluent. Different suitable

boundary conditions and initial conditions are selected for the computational domain and simulation is performed. Adiabatic boundary condition is declared to the cold end wall, compressor wall, all transfer line, valve and to the reservoir. A constant wall temperature is declared to the hot end heat exchanger and compressor heat exchanger. The system is operated with 25 bar mean charge pressure. To track the piston head velocity a DEFINE_CG_MOTION UDF is attached and dynamic mesh option is enabled. The initial operating temperature is chosen 300 K for an initial condition of operation. Helium is chosen as the working fluid, and assumed as viscosity is temperature dependent. The time step of 0.0005 s is selected for iteration and for well solution convergence inner step size 50 is considered. It takes above 20 days to achieve steady state with 8GB CPU configuration and 3.1 GHz processor RAM .

2.4. solution details and procedure

Suitable numerical scheme is required for better convergent during solution process. Axisymmetric, cell based second order implicit scheme, transient, cell based second order implicit scheme; physical velocity with segregated solver is considered for simulations. For the pressure velocity coupling, PISO algorithm along with PRESTO (Pressure Staggered Option) scheme is used. Appropriate under relaxation factors for pressure, for momentum and for energy are selected for the improved convergence. For the domain quad lateral cells are used. 10^{-6} is chosen field residual value for convergence of the discretized equations.

2.5. Grid variation test

A grid variation test is conducted to ensure the accuracy of the computational grid. Five different grid numbers are chosen for the verification of the grid accuracy test in the form of the cold end temperature of the PTRs. The various sizes of grids chosen for the numerical domain are 14742, 8734, 3986, 3147 and 2421 nodes. Fig.2 presents the cold end temperatures for the various grid number of the given computational domain. It can be conclude from the test that the grid size 3986 node is suitable for analysis. Hence, in the present work 3986 numbers of nodes are accepted to analyze the performance of the PTR.

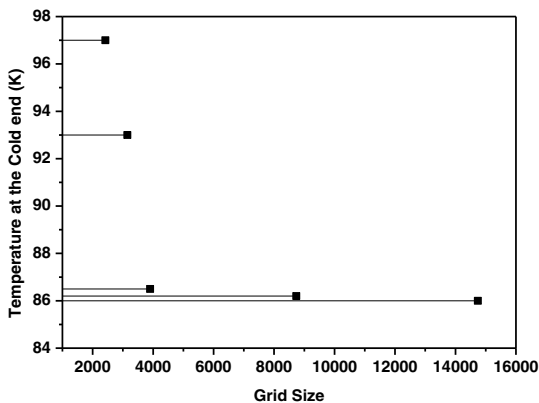


Fig.2 Temperature change with change of grid change

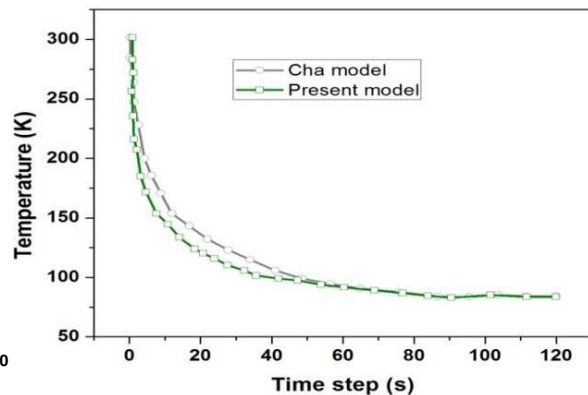


Fig.3 Model Validation plot among existing model and Cha et al. [14] model

For model validation the present numerical model results is compared with the Cha et al. [14] model and reported a good agreement between two models as shown in Fig. 3. The steady state temperature reached after 80 second which can be seen from the above figure. With 4200 numbers of grid Cha et al. [14] model achieved 87 K whereas the present model with 3986 number of nodes reached 86.4 K.

3. Results and Analysis

3.1. OPTR

After model validation the simulation conducted for OPTR model, shown in Fig. 1 (a) model as the DIPTR [16-18] model, shown in Fig. 1 (b) is complicated to solve using axisymmetric model. The procedure followed as mentioned above. A lower temperature of about 130 K is reported at the cold end of the OPTR taking the dimension from Antao et al. [15]. The temperature variation along the axial direction from after cooler wall to reserve presented in Fig. 4. It shows a decreasing temperature gradient from after cooler to cold heat exchanger then there is increase in temperature gradient to hot heat exchanger.

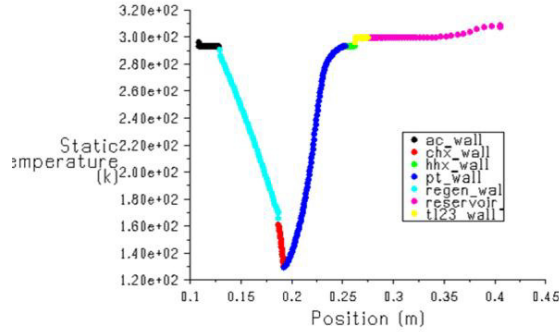


Fig.4 Temperature variation along axial direction of OPTR after steady state.

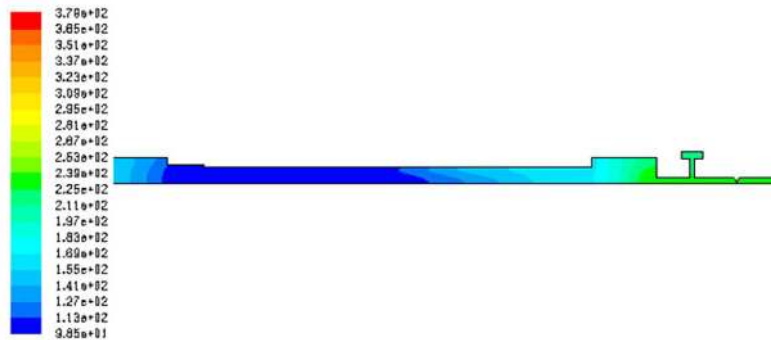


Fig.5 Contour showing the temperature of the MTPTR

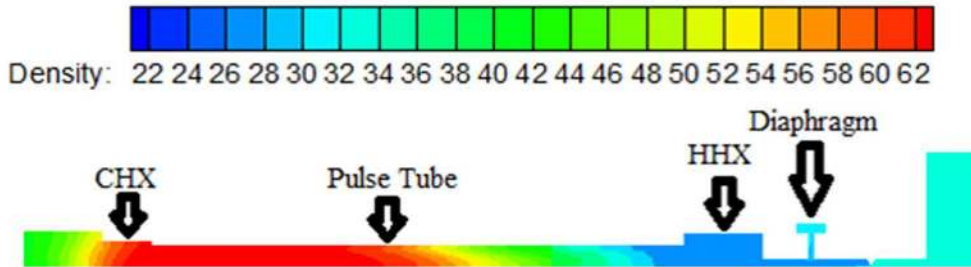


Fig. 6 Contour showing the density variation of the MTPTR

3.2. MPTR

The similar methodology and dimension are adopted for the MPTR analysis as chosen for the previous OPTR case. It is reported a 98 K temperature at the cold end and the contours for the MPTR model is shown in Fig. 5. The secondary compressor attached at the hot end is to provide a suitable phase shift mechanism between pressure and mass flow rate just similar to the by pass works for the DIPTR model. The secondary compressor will provide the same mass flow rate as the bypass gives. Proper setting of amplitude of the piston will control the mass flow rate to and from the hot end. Fig. 6 shows the density contour of the MPTR model. It shows that at the cold end high density where as hot end low density.

4. Conclusion

The proposed numerical investigation is to reduce the DC gas flow in a pulse tube refrigerator. An additional compressor is introduced at the hot end to break the bypass between hot end and after cooler as a result DC flow through the cycle stops. Helium is used as the working fluid and operating pressure ratio is 1.2. The results found that a below 100 K achieved using the proposed model where as a simple OPTR having same dimensions taken from [15] produce a temperature of about 128 K. Temperature instability is the main problem associated with DIPTR. From the present investigation it is reported that that, temperature stability is achieved near the cold end and produced an improved cooling effect at cold end comparison to OPTR. The experimental work on the proposed model will give a new era in the same field of research.

References

- [1] Hu JY, Luo EC, Wu ZH, Dai W, Zhu SL. Investigation of an innovative method for DC flow suppression of double-inlet pulse tube coolers. *Cryogenics* 2007;47:287–91.
- [2] Kanao K, Watanabe N, Kanazawa Y. A miniature pulse tube refrigerator for temperature below 100 K. *Cryogenics* 1994;30(ICEC 15 Suppl.):167–70.
- [3] Masuyama S, Kim YH, Park SJ, et al. Experimental research of Stirling type pulse tube refrigerator with an active phase control. *Cryogenics* 2006;46(5):385–90.
- [4] Rout, S.K., et al., Multi-objective parametric optimization of Inertance type pulse tube refrigerator using response surface methodology and non-dominated sorting genetic algorithm *Cryogenics* 62, 71–83, (2014).
- [5] Zhu S, Kakimi Y, Matsubara Y. Investigation of active-buffer pulse tube refrigerator. *Cryogenics* 1997;37(8):461–71.
- [6] Kaiser G, Brehm H, Wagner R, et al. Advantages of a four-valve pulse tube cryocooler for high-Tc, sensor operation. *Cryogenics* 1997;37(10):699–703.
- [7] Yang LW, Thummes G. High frequency two-stage pulse tube cryocooler with base temperature below 20 K. *Cryogenics* 2004;45(2): 155–9.
- [8] Pan, H., A. Hofmann, and L. Oellrich, Single-stage 4-valve and active buffer pulse tube refrigerators. *Cryogenics*, 2001. 41(4): p. 281–284.
- [9] Chen G, Qiu L, Zheng J, et al. Experimental study on a double orifice two-stage pulse tube refrigerator. *Cryogenics* 1997;37(5): 271–3.
- [10] Zhou Y, Han YJ. Pulse tube refrigerator research. In: *Proceedings of the 7th international cryogenic conference, Santa Fe*. 1992. p. 147–51.
- [11] Hu JY, Luo EC, Wu ZH, Dai W, Zhu SL. Investigation of an innovative method for DC flow suppression of double-inlet pulse tube coolers. *Cryogenics* 2007; 47:287–91.
- [12] Backhaus S, Swift GW. An acoustic streaming instability in thermoacoustic devices utilizing jet pumps. *J Acoust Soc Am* 03;113(3):1317–24.
- [13] Shiraiishi, M. and M. Murakami, Visualization of oscillating flow in a double-inlet pulse tube refrigerator with a diaphragm inserted in a bypass-tube. *Cryogenics*, 2012. 52(7–9): p. 410–415.
- [14] Cha JS, Ghiaasiaan SM. Multidimensional flow effects in pulse tube refrigerators. *Cryogenics* 2006, 46:658–665.
- [15] Antao D. S, Bakhtier Farouk, Experimental and numerical investigations of an orifice type cryogenic pulse tube refrigerator. *Applied Thermal Engineering* 50 (2013) 112–123.
- [16] Arablu, M.; Jafarian, A. “Investigation of synchronous effects of multi-mesh regenerator and double-inlet on performance of a Stirling-type pulse tube cryocooler,” *Cryogenic* 2013, 54, 1–9.
- [17] Arablu, M.; Jafarian, A. “A modified two-stage pulse tube cryocooler considering oscillating friction factor, multi-mesh regenerator and double inlet,” *Cryogenics* 2013, 58, 26–32.
- [18] Arablu, M.; Jafarian, A.; Deylami, P. “Numerical simulation of a two-stage pulse tube cryocooler considering influence of abrupt expansion/contraction joints,” *Cryogenics* 2013, 57, 150–157.